AMERICAN ACADEMY OF OPHTHALMOLOGY®

Study of Late-Onset Stargardt Type 1 Disease

Characteristics, Genetics, and Progression

Catherina H.Z. Li, MD,[1,2] Jeroen A.A.H. Pas, MD,[1,2] Zelia Corradi, MSc,[2,3,4] Rebekkah J. Hitti-Malin, PhD,[2,3,4] Anne Hoogstede, BSc,[1] Esmee H. Runhart, MD, PhD,[1,2] Patty P.A. Dhooge, MD, PhD,[1,2] Rob W.J. Collin, PhD,[2,3,4] Frans P.M. Cremers, PhD,[2,3,4] Carel B. Hoyng, MD, PhD[1,2]

Purpose: Late-onset Stargardt disease is a subtype of Stargardt disease type 1 (STGD1), defined by an age of onset of 45 years or older. We describe the disease characteristics, underlying genetics, and disease progression of late-onset STGD1 and highlight the differences from geographic atrophy.

Design: Retrospective cohort study.

Participants: Seventy-one patients with late-onset STGD1.

Methods: Medical files were reviewed for clinical data including age at onset, initial symptoms, and best-corrected visual acuity. A quantitative and qualitative assessment of retinal pigment epithelium (RPE) atrophy was performed on fundus autofluorescence images and OCT scans.

Main Outcome Measures: Age at onset, genotype, visual acuity, atrophy growth rates, and loss of external limiting membrane, ellipsoid zone, and RPE.

Results: Median age at onset was 55.0 years (range, 45−82 years). A combination of a mild and severe variant in ATP-binding cassette subfamily A member 4 (*ABCA4*) was the most common genotype (n = 49 [69.0%]). The most frequent allele, c.5603A→T (p.Asn1868Ile), was present in 43 of 71 patients (60.6%). No combination of 2 severe variants was found. At first presentation, all patients have flecks. Foveal-sparing atrophy was present in 33.3% of eyes, whereas 21.1% had atrophy with foveal involvement. Extrafoveal atrophy was present in 38.9% of eyes, and no atrophy was evident in 6.7% of eyes. Time-to-event curves showed a median duration of 15.4 years (95% confidence interval, 11.1−19.6 years) from onset to foveal involvement. The median visual acuity decline was −0.03 Snellen decimal per year (interquartile range [IQR], −0.07 to 0.00 Snellen decimal; 0.03 logarithm of the minimum angle of resolution). Median atrophy growth was 0.590 mm^2/year (IQR, 0.046−1.641 mm^2/year) for definitely decreased autofluorescence and 0.650 mm^2/year (IQR, 0.299−1.729 mm^2/year) for total decreased autofluorescence.

Conclusions: Late-onset STGD1 is a subtype of STGD1 with most commonly 1 severe and 1 mild *ABCA4* variant. The general patient presents with typical fundus flecks and retinal atrophy in a foveal-sparing pattern with preserved central vision. Misdiagnosis as age-related macular degeneration should be avoided to prevent futile invasive treatments with potential complications. In addition, correct diagnosis lends patients with late-onset STGD1 the opportunity to participate in potentially beneficial therapeutic trials for STGD1.

Financial Disclosure(s): The author(s) have no proprietary or commercial interest in any materials discussed in this article. *Ophthalmology 2024;131:87-97 © 2023 by the American Academy of Ophthalmology. This is an open access article under the CC BY license (http://creativecommons.org/licenses/by/4.0/).*

Supplemental material available at www.aaojournal.org.

Stargardt disease type 1 (STGD1) (Online Mendelian Inheritance in Man identifier, 248200), caused by biallelic pathogenic variants in the ATP-binding cassette subfamily A member 4 (*ABCA4*) gene, originally was considered a juvenile macular degeneration with profound vision loss.[1,2] However, a much wider variation of clinical phenotypes ranging from early onset with fast progressive cone−rod dystrophy to onset later in life with mild retinal degeneration or a bull's-eye maculopathy is seen.[3,4] This coincides with great allelic heterogeneity, with more than 2200 *ABCA4* (Online Mendelian Inheritance in Man identifier, 601691) variants reported (lovd.nl/ABCA4; accessed on January 23, 2023) to date.[5,6] Dysfunction of the ABCA4 protein results in accumulation of toxic N-retinylidene-N-retinyl-ethanolamine lipofuscin in the retinal pigment epithelium (RPE) cells and eventually leads to irreversible destruction of photoreceptor cells.[2]

The residual function of the ABCA4 protein is correlated with disease severity of STGD1.[3,7] When 1 of the 2 causal

https://doi.org/10.1016/j.ophtha.2023.08.011
ISSN 0161-6420/23

ABCA4 variants is considered to have a milder effect, leaving more residual protein function, a milder phenotype and late onset of disease is seen.[8] In these patients, relative sparing of the fovea is a typical feature, which starts as parafoveal atrophic lesions that subsequently merge, leaving a peninsula-like intact RPE.[9,10] When the disease progresses, the fovea is encircled completely by RPE atrophy, and eventually the fovea also becomes involved.[11]

Late-onset STGD1 makes up an increasing proportion of patients with newly diagnosed STGD1, that is, 33% from 2014 through 2018 compared with 19% from 2004 through 2009 in the Netherlands.[12] In our first publication, almost half of the patients harbored monoallelic variants, and therefore genetically were unsolved.[9] With improved genotyping techniques, which identified mild deep-intronic variants such as c.769-784C→T and c.4253+43G→A,[13,14] and the reappraisal of coding variants with a high allele frequency in the general population (c.5603A→T, p.Asn1868Ile),[15] a second variant could be identified in the previously unsolved cases, contributing to an increased diagnosis of late-onset STGD1 resulting from genetic confirmation.

Nonetheless, late-onset STGD1 remains underdiagnosed. This is apparent because 22% of patients with the currently known late-onset STGD1 were previously misdiagnosed with age-related macular degeneration (AMD).[8,12] Given that AMD is a much more prevalent diagnosis, having similar phenotypic features, and similar age at onset, misdiagnosis in daily clinical practice is understandable.[9,12] Misdiagnoses are undesirable not only for clinical understanding, but especially regarding patients with STGD1, who may receive unnecessary invasive treatments targeted at another disease (e.g., pegcetacoplan injection for AMD) or who miss the opportunity to participate in upcoming clinical trials with a potentially effective treatment.

To date, only a small group of patients with late-onset STGD1 have been described in the literature. These patients also could be eligible for upcoming therapeutic clinical trials for STGD1. For this reason, it is necessary to have a detailed clinical and genotypic description to identify these patients adequately. In the current study, we describe the phenotypic appearance, disease progression, and genetic background of a uniquely large cohort of patients with late-onset STGD1.

Methods

Patients

The Radboud University Medical Center (Nijmegen, The Netherlands) STGD1 database currently comprises data from 506 patients who received a clinical diagnosis of STGD1 between 1952 and 2022. For this retrospective study, we included patients who experienced first symptoms at 45 years of age or older and who carried at least 1 likely pathogenic or pathogenic *ABCA4* variant. Asymptomatic patients were included when they presented with macular abnormalities at 45 years of age or older because they will develop symptoms later in the disease course. Monoallelic patients were included only when the clinical phenotype was typical for STGD1 through assessment by an experienced ophthalmologist (C.B.H.) who specializes in STGD1. Patients with ocular comorbidities other than cataract were excluded. The study was performed in adherence to the tenets of the Declaration of Helsinki. The institutional ethics committee, CMO Radboud University Medical Center, ruled that approval was not required for this study and waived the requirement for informed consent (file number, 2022-15718).

Genetic Analyses

Genotyping was performed between 2002 and 2022. Blood was drawn and DNA was isolated for genetic analysis as part of routine patient care. *ABCA4* variants were identified through allele-specific primer extension microarray analysis, *ABCA4* exon and splice site sequencing, or whole exome sequencing. Additional single-molecule molecular inversion probes (smMIPs) double-tiling targeting the entire *ABCA4* gene[14]; smMIPs targeting at exons, splice sites, and published pseudoexons in genes associated with macular diseases[16]; or HaloPlex-based sequencing (Agilent Technologies)[13] of the *ABCA4* gene were performed in 48 of 71 patients. Severity of the *ABCA4* variants was classified as either mild, moderate, or severe.[6] Variant c.5603A→T is considered a mild-incomplete penetrant variant based on earlier studies.[8,17] Phasing of the genetic variants was determined either through segregation analysis (n = 13) or based on the most frequently found combination.

Single-Molecule Molecular Inversion Probe-Based *ABCA4* Sequence Analysis and Data Processing

DNA samples were quantified, diluted to 15 to 25 ng/μl, and DNA integrity was assessed using agarose gel electrophoresis. Thirty-eight samples were screened using the smMIPs probe pool with 3866 smMIPs with a 110-nucleotide capture region, screening the entire *ABCA4* gene as described previously.[14] Two samples were screened using the macular degeneration-smMIPs panel comprising 17 394 smMIPs capturing 105 inherited macular degeneration and AMD-associated genes[16] with probes with a capture region of 225 nucleotides. SmMIP runs were performed on a NextSeq500 (Illumina) platform using high-output kits (approximately 400 million reads) and NovaSeq6000 (Illumina) platform using SP reagent kits version 1.5 (300 cycles) and custom sequencing primers for the *ABCA4* and macular degeneration-smMIPs panel, respectively. Variants were mapped using an in-house bioinformatics pipeline as described previously.[14] Known *ABCA4* variants, previously reported in the literature and listed in the Leiden Open (source) Variation database (https://databases.lovd.nl/shared/genes/ABCA4; accessed May 15, 2022), were identified. Novel causative variants were assessed using the American College of Medical Genetics and Genomics classification, ascertained using the Franklin by Genoox platform (https://franklin.genoox.com/; accessed December 15, 2022). Novel variants putative of altering splicing were assessed using SpliceAI predictions.[18]

Data Collection

Clinical data, including sex, age at onset, age at diagnosis, genotype, and initial symptoms, were retrieved from medical files. Best-corrected visual acuity, fundus autofluorescence (FAF) imaging, and spectral-domain OCT imaging from all available visits were collected. A total of 228 FAF and 260 OCT scans were available. Fluorescein angiography and indocyanine green

angiography are not considered part of standard care for patients with STGD1, and therefore were not included in the study.

Quantitative Assessment of Imaging

Retinal atrophy area was measured in square millimeters on 30° FAF images using the Heidelberg Regionfinder (Heidelberg Engineering) semiautomatic grading software. When atrophy exceeded the borders of 30°, the 55° image was used. Retinal pigment epithelium atrophy was defined as either definitely decreased autofluorescence (DDAF; atrophic area 90% as dark as the optic nerve head) or questionably decreased autofluorescence (atrophic area 50%−90% as dark as the optic nerve head).[19] The sum of both was defined as total decreased autofluorescence (TDAF).

The loss of the retinal sublayers ellipsoid zone (EZ), external limiting membrane (ELM), and RPE was measured on transfoveal spectral-domain OCT B-scans using the built-in OCT distance measurement tool in Heyex (Heidelberg Engineering). When normal retinal tissue interrupted the layer loss, the sum (in micrometers) of the multiple segments of layer loss was used. Images with atrophy or layer loss exceeding the borders of the image were excluded because the total amount could not be determined. Being a manually performed measurement, the average of the measurements by 2 independent graders (A.H., J.A.A.H.P.) was used.

Qualitative Assessment of Imaging

Atrophy with foveal sparing is one of the key features of late-onset STGD1. We therefore distinguished 4 disease stages based on the phenotype at first and last presentation: (1) no atrophy with intact fovea, (2) extrafoveal (but no fovea encircling atrophy), (3) a typical foveal-sparing phenotype in which atrophy encircled the fovea by 180° or more, and (4) foveal involvement (Fig S1, available at www.aaojournal.org).[10] We determined the start of foveal sparing and foveal involvement by grading all available images. In addition, images were graded for presence of flecks and atrophy was graded to be either mottling or well demarcated.

Statistical Analysis

Statistical analyses were performed using SPSS software version 27 (IBM). The first presentation analysis focused exclusively on the initial visits that occurred within 5 years after the onset of symptoms. This selection criterion was implemented to account for patients undergoing first imaging several years after the initial visit to the ophthalmologist because of the limited availability of these imaging techniques during earlier periods. A total of 90 FAF and 85 OCT scans qualified for the first presentation analysis. Mean progression rates per year for various parameters were calculated for the subgroup of patients with follow-up data using data from the first and last available visits. Atrophy area was measured and expressed in square millimeters. To facilitate comparison with prior studies, atrophy progression rates were expressed as area growth in square millimeters, root-(π)-transformed radius in millimeters ($\sqrt{\frac{area}{\pi}}$), and (square) root-transformation in millimeters ($\sqrt{area}$). These 3 values were provided to align with previous literature, with root transformation being the preferred unit. Time-to-event analyses were performed using Kaplan-Meier curves. Intereye correlation was assessed using intraclass correlations. A nonnormal distribution was found, and values were expressed as median and interquartile range (IQR). A P value of < 0.05 was defined as statistically significant.

Results

We identified 103 patients with an age at onset of 45 years or older from the STGD1 database, 17 of whom did not have at least 1 likely pathogenic or pathogenic *ABCA4* variant. These patients received a clinical diagnosis of STGD1 and exhibited a phenotype similar to that of the study cohort. However, their genetic status is not resolved (yet) or they did not undergo genotyping because of having been diagnosed a long time ago. Patients were excluded for the following reasons: no imaging (n = 11), ocular comorbidity (n = 3; central retinal vein occlusion [n = 1], Graves' ophthalmopathy [n = 1], and amblyopia [n = 1]), and medical file unavailable (n = 1). A total of 71 patients were included in this study (Table 1), of whom 69 patients harbored 2 likely pathogenic or pathogenic variants in the *ABCA4* gene. The median age at onset was 55.0 years (range, 45−82 years), and 49.3% were female. The median age at diagnosis was 59.0 years (IQR, 53.0−64.5 years). Follow-up data were available for 60 patients, with a median follow-up duration of 4.3 years (IQR, 2.2−6.6 years) based on FAF imaging findings. Because of the retrospective nature of the study, slight discrepancies exist for the follow-up duration among best-corrected visual acuity, FAF, and OCT imaging.

First Presentation

Median disease duration at first presentation was 1.7 years (IQR, 1.2−3.0 years). The most common initial symptom was a self-reported decrease in visual acuity (n = 38 [70.4%]). Six patients (11.1%) were asymptomatic at the time of diagnosis (Table 2). A typical phenotype for late-onset STGD1 is presented in Figure 2. All eyes except for 1 eye (n = 89 [98.9%]) showed flecks on the first available FAF imaging, mainly located in the macular area (n = 31 [34.4%]) and posterior pole (n = 41 [45.6%]; Table S3, available at www.aaojournal.org). Among the eyes, 33.3% (n = 30) showed foveal sparing with atrophy encircling the fovea by 180° or more and 21.1% (n = 19) showed atrophy with foveal involvement. No atrophy was present in 6 eyes (6.7%). Best-corrected visual acuity at first presentation was 0.80 Snellen decimal (IQR, 0.53−1.00 Snellen decimal; 0.10 logarithm of the minimum angle of resolution [logMAR]; IQR, 0.00−0.28 logMAR). Median atrophy area DDAF was 0.16 mm^2 (IQR, 0.0−3.68 mm^2) and TDAF was 1.86 mm^2 (IQR, 0.79−5.95 mm^2). Median retinal layer loss was 1054 μm (IQR, 158−2208 μm), 1648 μm (IQR, 718−2639 μm), and 983 μm (IQR, 46−2128 μm) for ELM, EZ, and RPE, respectively (Table 1).

Genotype

The most frequently identified genotype was a combination of a mild variant together with a severe variant (n = 49 [69.0%]; Table S4, available at www.aaojournal.org), 28 of which concerned a mild incompletely penetrant variant. Other combinations included severe plus moderate (n = 5 [7.0%]), severe with a variant of unknown significance (n = 4 [5.6%]), moderate plus mild (n= 4 [5.6%]), mild plus mild (n = 3 [4.2%]), severe with a second variant not found (n = 2 [2.8%]), severe with a variant of unknown severity (n = 1 [1.4%]), moderate plus mild-moderate (n = 1 [1.4%]), mild-moderate plus mild (n = 1 [1.4%]), and mild plus benign-mild (n = 1 [1.4%]). No severe plus severe combinations were found.

The most frequent allele was c.5603A→T (p.Asn1868Ile) (n = 28 [19.7%]), followed by c.768G→T (n = 15 [10.6%]) and c.5461-10T→C;5603A→T (n = 14 [9.9%]). The c.5603A→T variant was present in 43 of 71 patients (60.6%; Table S5, available at www.aaojournal.org). In 23 patients, this variant was in *trans* (i.e., on the other allele), with a severe variant and in 2 patients

Table 1. Patient and Eye Characteristics at First Presentation

Characteristic	No. or No. (%)	Median (Interquartile Range)
Female sex	35 (49.3)*	
Age at onset (yrs)	71*	55.0 (50.0–61.0)
Age at diagnosis (yrs)	69*	59.0 (53.0–64.5)
Delay in diagnosis (yrs)	69*	1.0 (0.0–4.0)
Disease duration at first presentation (yrs)		
FAF	40*	1.7 (1.2–3.0)
OCT	43*	1.7 (1.2–3.1)
VA	50*	1.3 (0.3–2.2)
First presentation		
DDAF (mm^2)	90†	0.16 (0.00–3.68)
QDAF (mm^2)	90†	0.90 (0.38–2.00)
TDAF (mm^2)	90†	1.86 (0.79–5.95)
ELM loss (μm)	84†	1054 (158–2208)
EZ loss (μm)	84†	1648 (718–2639)
RPE loss (μm)	85†	983 (46–2128)
Visual acuity		
logMAR	100†	0.10 (0.00–0.28)
Snellen decimal	100†	0.80 (0.53–1.00)

DDAF = definitely decreased autofluorescence; ELM = external limiting membrane; EZ = ellipsoid zone; FAF = fundus autofluorescence; logMAR = logarithm of the minimum angle of resolution; QDAF = questionably decreased autofluorescence; RPE = retinal pigment epithelium; TDAF = total decreased autofluorescence; VA = visual acuity.
*Patients.
†Eyes.

in *trans* with a variant of moderate severity. In 18 patients, the c.5603A→T variant formed a complex allele with c.2588G→C (n = 5), c.5461-10T (n = 11), c.769-784C→T (n = 2), and c.5537T→C (n = 1).

A positive family history was found for 18 families, 3 patients of which included a sibling with a much earlier age at onset of symptoms (Table S5). In 2 families, 2 unaffected siblings carried the same *ABCA4* variants as their affected siblings. However, they did not exhibit any retinal abnormalities attributed to STGD1 and experienced no symptoms at the ages of 51 and 70 years, as assessed by an ophthalmologist specializing in retinal diseases (C.B.H.; Fig S3, available at www.aaojournal.org).

Disease Progression

After a median follow-up duration of 5.4 years (IQR, 2.2–11.7 years), best-corrected visual acuity deteriorated to a median of 0.50 Snellen decimal (IQR, 0.10–0.98 Snellen decimal; 0.3 logMAR; IQR, 0.01–1.00 logMAR). The median visual acuity decline was −0.03 Snellen decimal/year (IQR, −0.07 to 0.00 Snellen decimal/year; 0.03 logMAR; IQR, 0.00–0.08 logMAR). Time-to-event analysis yielded a median of 9.0 years (95% CI, 4.6–13.4 years), 12.0 years (95% CI, 9.6–14.4 years), and 15.0 years (95% CI, 12.9–17.1 years) from onset to reach mild (≤ 0.5 Snellen decimal; ≥ 0.3 logMAR), moderate (≤ 0.3 Snellen decimal; ≥ 0.5 logMAR), and severe (≤ 0.1 Snellen decimal; ≥ 1.0 logMAR) visual impairment, respectively (Fig 4).

Table 2. Initial Symptoms

Initial Symptom	No. of Eyes (%)
Decrease in visual acuity	38 (70.4)
Metamorphopsia	15 (27.8)
Nyctalopia	7 (13.0)
Paracentral scotoma	9 (16.7)
Mouches volantes	4 (7.4)
Subjective difference in color perception	4 (7.4)
Diplopia	1 (1.9)
Asymptomatic at first presentation	6 (11.1)

The reported initial symptoms for 54 patients.

The radius of the atrophy grew by 0.097 mm/year (IQR, 0.042–0.156 mm/year; root-transformed equivalent, 0.172 mm/year) for DDAF and 0.098 mm/year (IQR, 0.054–0.141 mm/year; root-transformed equivalent, 0.174 mm/year) for TDAF. This corresponds to an area growth of 0.590 mm^2/year (IQR, 0.046–1.641 mm/year) for DDAF and 0.650 mm^2/year (IQR, 0.299–1.729 mm/year) for TDAF. The progression rate of ELM loss was 186 μm/year (IQR, 87–306 μm/year), that of EZ loss was 231 μm/year (IQR, 119–339 μm/year), and that of RPE loss was 182 μm/year (IQR, 92–328 μm/year; Table 6).

Left and right eyes of a patient were well correlated at first presentation for all the outcome measurements, calculated using intraclass correlation coefficients (Table S7, available at www.aaojournal.org). Progression was only moderately or well-correlated for the atrophy outcome of DDAF, the retinal layer loss outcomes of EZ loss and RPE loss, and visual acuity decline.

Of all the eyes with atrophy, 31.9% (n = 30) showed mottled atrophy and 68.1% (n = 64) showed well-demarcated atrophy. At the last visit, flecks were located mostly in the posterior pole and middle periphery (81.8%; Table S3). In 18.1% of eyes, the flecks remained limited to the macula. During follow-up (n = 94), a total of 19 eyes progressed from foveal sparing to foveal involvement, and 40.7% of the eyes (n = 57) showed foveal sparing at some point during the disease course (Fig 5). For the remaining eyes, the presence of foveal sparing could not be determined because of foveal involvement (30.7% [n = 43]) at the first available imaging or because of extrafoveal atrophy (27.1% [n = 38]) at last presentation, in which the follow-up might not have been long enough to observe foveal sparing. Two

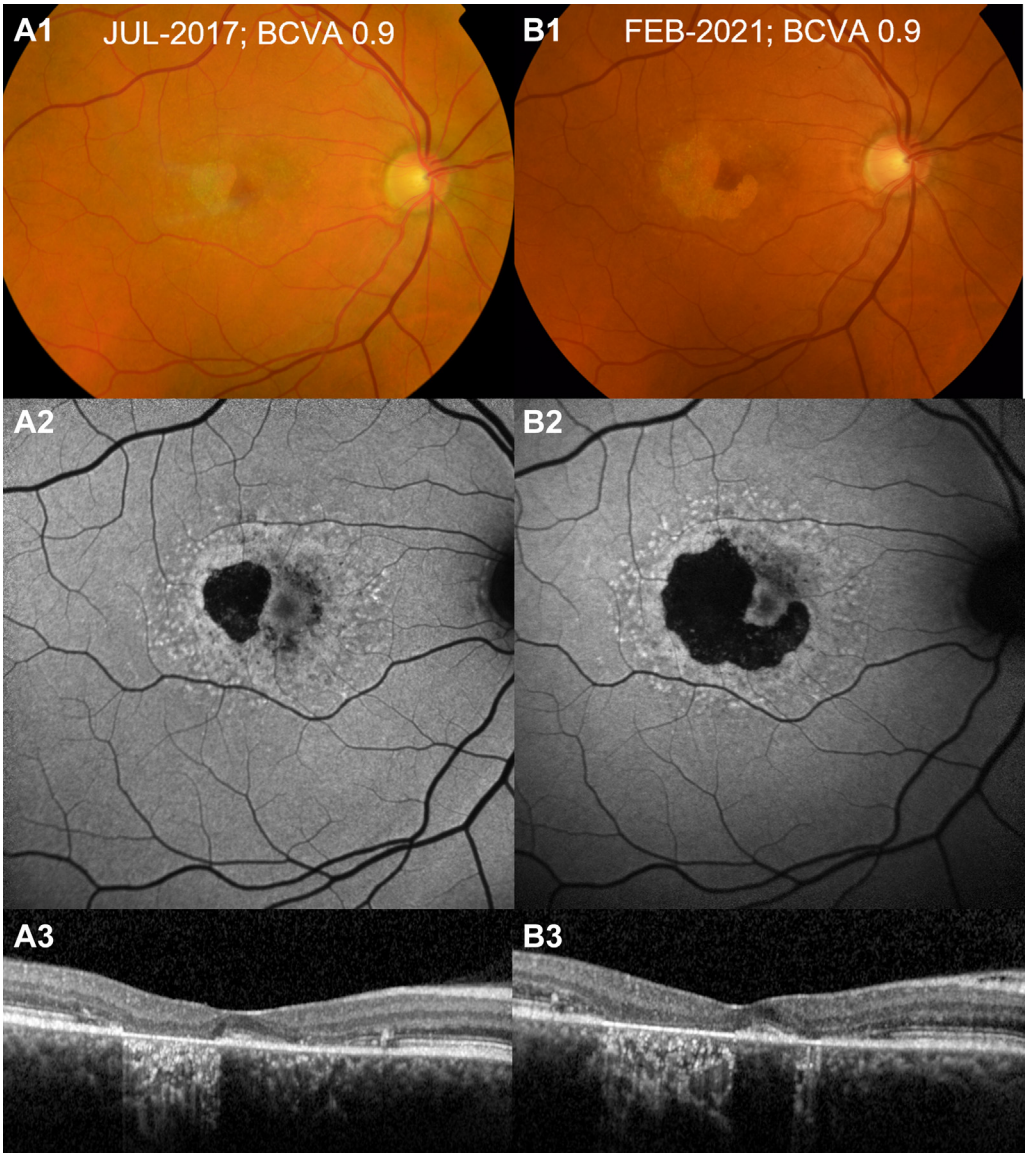

Figure 2. Multimodal imaging of a typical phenotype of late-onset Stargardt disease type 1 (STGD1). Imaging of the right eye of a male patient, onset of symptoms at 58 years of age, carrying 2 *ABCA4* variants (c.3322C→T and c.5603A→T), obtained (**A**) at the first visit (3 years since onset) and (**B**) at the last visit with 3.6 years of follow-up: color fundus photographs (**A1**, **B1**), fundus autofluorescence images (**A2**, **B2**), and foveal OCT scans (**A3**, **B3**). Although atrophy growth is significant, best-corrected visual acuity (BCVA) remained stable at 0.9 Snellen decimal (0.05 logarithm of the minimum angle of resolution) because of foveal sparing.

eyes of 1 patient (1.4%) progressed from extrafoveal atrophy encircling the fovea by less than 180° to atrophy with foveal involvement over 7 years, without any available imaging during the intermediate period. Time-to-event analyses yielded a median of 7.4 years (95% CI, 4.7−10.1 years) from onset for foveal sparing and a median of 15.4 years (95% CI, 11.1−19.6 years) for foveal involvement (Fig 6).

Discussion

Although awareness has increased over the years, we believe that patients with late-onset STGD1 remain underdiagnosed. It is clear that knowledge of this subtype is still lacking, as demonstrated through recent publications of case reports on presumably rare cases of STGD1 with late onset.[20,21] A major discrepancy is seen between the genetically estimated prevalence of STGD1 cases of 1 in 6578 and the point prevalence of 1 in 19 000 to 22 000 individuals found in The Netherlands.[12,22] Assuming these numbers and a population of 17 million people, approximately 2500 patients with STGD1 should be present in The Netherlands, although only 800 are known. Therefore, 1700 patients are unaccounted for. We hypothesize that this gap is made up of around 1000 nonaffected individuals harboring *ABCA4* variants with reduced penetrance (i.e., when not all individuals carrying

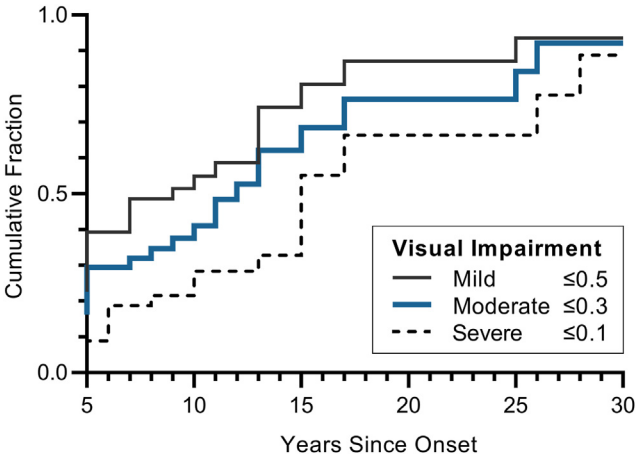

Figure 4. Time-to-event curves showing the cumulative fraction of patients with Stargardt disease type 1 reaching the following World Health Organization category of visual impairment: mild (≤ 0.5 Snellen decimal; ≥ 0.3 logarithm of the minimum angle of resolution [logMAR]), moderate (≤ 0.3 Snellen decimal; ≥ 0.5 logMAR), and severe (≤ 0.1 Snellen decimal; ≥ 1.0 logMAR) visual impairment.

the variant[s] show disease expression), and that the remaining 700 patients are patients with late-onset STGD1 whose disease is undiagnosed or misdiagnosed with phenocopies.[8,12] In the United States, this translates roughly to 14 000 missing patients with late-onset STGD1, clearly demonstrating the scale and importance of this underrepresented group. Therefore, we have provided a detailed description of a large cohort of patients with late-onset STGD1, including disease characteristics, genetic background, and disease progression.

Table 6. Disease Progression per Year for Atrophy and Visual Acuity

Disease Progression per Year	No. of Eyes	Median (Interquartile Range)
DDAF (mm)	90	0.097 (0.042–0.156)
QDAF (mm)	90	0.024 (−0.005 to 0.051)
TDAF (mm)	90	0.098 (0.054–0.141)
ELM loss (μm)	77	186 (87–306)
EZ loss (μm)	77	231 (119–339)
RPE loss (μm)	80	182 (92–328)
Visual acuity		
logMAR	108	0.03 (0.00–0.08)
Snellen decimal	108	−0.03 (−0.07 to 0.00)

DDAF = definitely decreased autofluorescence; ELM = external limiting membrane; EZ = ellipsoid zone; IQR = interquartile range; logMAR = logarithm of the minimum angle of resolution; QDAF = questionably decreased autofluorescence; RPE = retinal pigment epithelium; TDAF = total decreased autofluorescence.
The median progression rates for atrophy and visual acuity per year, including the interquartile ranges, in millimeters per micrometers. Questionably decreased autofluorescence and DDAF plus QDAF are displayed as radius transformations of the areas of atrophy in millimeters. Based on a median follow-up duration of 4.3 years (IQR, 2.2–6.6 years) for DDAF, QDAF, and TDAF; 4.5 years (IQR, 2.2–6.4 years) for ELM, EZ, and RPE loss; and 5.4 years (IQR, 2.2–11.7 years) for visual acuity.

Genotype

Late-onset STGD1 is on the milder end of the STGD1 phenotype spectrum, and likewise, milder combinations of a severe and a mild *ABCA4* variant are seen with supposedly more residual ABCA4 protein function. No combinations of 2 severe variants were found. In addition, notably hypomorphic variants (i.e., a mutation that leads to partial loss of normal gene function) with variable penetrance are abundant in our cohort. This finding is consistent with the study by Lee et al,[23] in which they reported that both rare and common hypomorphic alleles frequently were found in patients with mild disease with delayed onset and foveal sparing. These variants lead to variable disease expression when in *trans* with mainly severe *ABCA4* variants. c.5603A→T (p.Asn1868Ile), a hypomorphic variant associated with late onset, was present in 60.6% of the patients with late-onset STGD1 in this study.[8,24] The mild founder variant c.2588G→C p.[Gly863Ala,delGly863] is completely penetrant when in *cis* with c.5603A→T and in *trans* with a severe or null allele.[15] In the present cohort, 3 biallelic patients carrying c.2588G→C did not harbor the c.5603A→T variant, which may suggest that its role could be similar to that of c.5603A→T. For this, unaffected siblings of probands carrying this variant should be tested genetically to investigate the possibility of nonpenetrance.

According to the genotype–phenotype correlation model introduced by Cremers et al[7] in 1998 and the updated versions,[5,25] in which the residual *ABCA4* function inversely corresponds with disease severity, a severe plus moderate combination causes a severe phenotype with early onset. In the present cohort, 5 patients carry this combination. In contrast, our cohort also includes patients with late-onset STGD1 with 2 mild variants and monoallelic patients, a genotype that, according to the model, does not cause disease. As a recessive disease, it must be assumed that 50% or more of the normal ABCA4 protein activity will not lead to disease. However, modifiers can influence the tolerance for a reduced ABCA4 protein level. Therefore, it is certainly possible that the presence of a set of modifiers with negative or protective effects (either genetic or environmental) influence the expression and penetrance of the disease, in particular in patients with combinations of mild plus moderate and mild plus mild variants. Considering that, in some families, siblings who carry the same *ABCA4* variants and were raised in a similar environment, and yet show substantial phenotypic discordance and variability in age at onset of symptoms, the role of genetic modifiers is more likely than environmental factors.[26]

We deliberately chose to include these patients with a very typical STGD1 phenotype but who are monoallelic or harbor *ABCA4* variants that together are theoretically too mild to cause disease expression. Strictly speaking, STGD1 is a term exclusively reserved for patients with STGD1 carrying disease-causing *ABCA4* variants in both gene copies. Considering this definition, the present cohort includes 55 of 71 patients with STGD1 (77.5%). In the past, STGD1 could be confirmed genetically in less than 50% of patients with a convincing STGD1 phenotype, and this

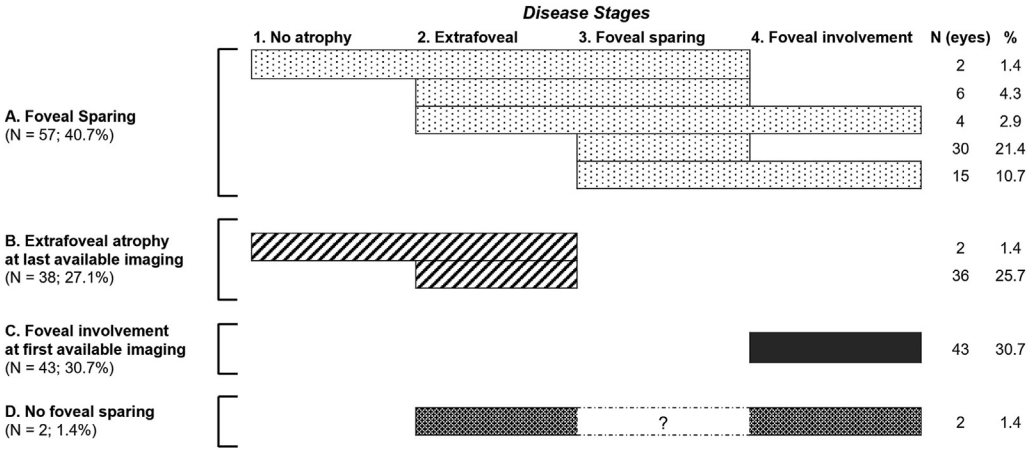

Figure 5. Graph showing disease progression through various disease stages in late-onset Stargardt disease type 1. **A**, Fifty-seven eyes (40.7%) showed foveal sparing at some point during the disease course. **B**–**D**, The eyes without foveal sparing included those with atrophy that remained extrafoveal throughout follow-up (n = 38 [27.1%]) (**B**), those with atrophy with foveal involvement at the first available imaging (n = 43 [30.7%]) (**C**), and 2 eyes of 1 patient (1.4%) that progressed from extrafoveal atrophy to atrophy with foveal involvement in 7 years without imaging available in between (**D**). This patient may have experienced foveal sparing.

disease was proposed by some even to belong to a subtype of AMD.[9,27] Although the genetic solve rate has improved substantially over the past decade, new variants are still being discovered because of advancements in sequencing technology. Therefore, we present these patients as part of the cohort with late-onset STGD1 assuming that, in time, the STGD1 diagnosis also can be confirmed genetically in these patients.

Phenotype

We previously described 13 patients with STGD1 with foveal sparing, most of whom received a diagnosis of late-onset STGD1, suggesting that foveal sparing is a main feature in late-onset STGD1.[11] In a cohort of patients harboring c.5603A→T (p.Asn1868Ile), a consistent phenotype was seen with later onset and relative foveal sparing.[24] In the current cohort, 40 eyes (70.2%) with foveal sparing carried the p.Asn1868Ile variant. Of the eyes with this variant in *trans* with a severe variant, 19 eyes (41.3%) showed foveal sparing during the disease course.

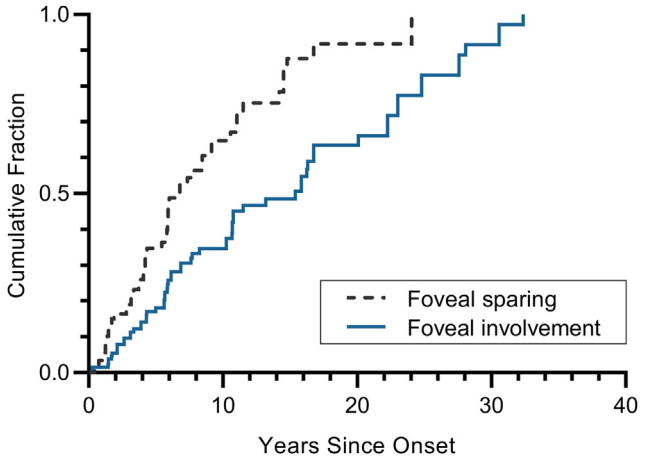

Figure 6. Time-to-event curves showing the cumulative fraction of patients with Stargardt disease type 1 reaching foveal-sparing atrophy and atrophy with foveal involvement.

The fovea contains the highest density of cones and is responsible for central vision.[28] Visual acuity is relatively well preserved when foveal sparing is present. Therefore, it is of clinical importance to know when parafoveal atrophy will grow inward and will affect the foveal tissue. In the current cohort, foveal sparing occurred in 33.3% of the patients at first presentation. Providing a precise prognosis regarding significant visual decline resulting from foveal involvement is challenging. Survival curves analysis shows that it takes a median time of 15.4 years from onset of symptoms for the atrophy to involve the fovea. Foveal sparing also is seen in some older patients (median age, 60 years) with other retinal dystrophies, including AMD, central areolar choroidal dystrophy, mitochondrial retinal dystrophy, and pseudo-Stargardt disease.[29] Although foveal sparing is found in a limited number of these patients, nearly all patients with late-onset STGD1 have shown foveal sparing at some point during the disease course. In the remaining patients, the presence of foveal sparing unfortunately could not be determined because of the retrospective nature of the study. This includes patients with foveal involvement on the first available imaging and patients with extrafoveal atrophy who may still develop foveal sparing atrophy later in the course of the disease. One patient had an unobserved interval of 7 years between the presence of extrafoveal atrophy and the

development of atrophy with foveal involvement. It is probable that this patient experienced foveal sparing during that unobserved period.

Disease Progression

In the literature, a great variation of growth rates of the atrophic lesions in STGD1 is reported, ranging from 0.39 to 1.84 mm^2/year.[30,31] Shen et al[32] performed a meta-analysis in 564 eyes from 7 studies and found a radius-transformed atrophy progression rate of 0.104 mm/year for the general STGD1 population. We found a progression rate of 0.097 for DDAF and 0.098 mm/year for TDAF in patients with late-onset STGD1, with an intereye correlation of intraclass correlation coefficient of more than 0.8 for all parameters (ELM, EZ, RPE, DDAF, and TDAF) at first presentation and only moderate or well-correlated intereye correlations (intraclass correlation coefficient, > 0.7) for the atrophy progression. This suggests that atrophy progression is quite similar in a patient's 2 eyes. The rate of growth of atrophic lesions seems to be similar in late-onset STGD1 compared with general STGD1, whereas visual decline is slow (−0.03 Snellen decimal/year; 0.03 logMAR). This suggests that atrophic lesions in late-onset STGD1 grow more outward than centrally, leaving the fovea intact longer. Although most patients with late-onset STGD1 show well demarcated RPE atrophy, one-third demonstrate mottled atrophy, that is, poorly demarcated, questionably decreased autofluorescent atrophy. This type is more difficult to quantify in a clinical trial.

Similarities to Age-Related Macular Degeneration with Geographic Atrophy

In the current era with upcoming clinical trials and promising treatment options, correct diagnosis is essential. Many phenocopies exist, like central areolar choroidal dystrophy caused by variants in *PRPH2* or maternally inherited diabetes and deafness caused by mutations in the mitochondrial DNA. However, AMD is the biggest distractor when diagnosing late-onset STGD1, with 22% of patients with late-onset STGD1 previously receiving a misdiagnosis as AMD with geographic atrophy (GA).[12] Considering the fact that AMD is the leading cause of blindness in the elderly,[33] this misdiagnosis is very credible because of comparable age at onset of symptoms and similar fundus abnormalities.[34]

Clinical trials targeting AMD naturally exclude patients with inherited retinal diseases. However, given the resemblance of AMD with GA to late-onset STGD1, it cannot be ruled out that patients with STGD1 are included unintentionally in these clinical trials, such as the pegcetacoplan trials in which routine genetic testing was not performed (ClinicalTrials.gov identifiers, NCT04770545, NCT03777332, NCT02503332, NCT03525613, and NCT03525600). Having gained Food and Drug Administration approval, pegcetacoplan may be administered to patients with late-onset STGD1, which not only provides no benefit, but also is accompanied by an unnecessary risk of complications. Therefore, differentiation between STGD1 and AMD with GA not only is essential for genetic and prognostic counseling, but also is of particular importance in the current era where new, promising therapeutics are emerging.

Age-related macular degeneration and late-onset STGD1 can be distinguished based on multimodal imaging (Fig 7). First, STGD1 flecks are irregularly shaped, as opposed to drusen, which are round. Second, drusen appear conspicuously yellow on color fundus photography, in contrast to flecks, which are slightly yellow and less prominently visible. On FAF imaging, the lipofuscin-rich STGD1 flecks are very notably hyperautofluorescent. Drusen, containing a variety of lipids and proteins and limited amounts of lipofuscin, are considerably less reflective, appearing mildly hyperautofluorescent to normoautofluorescent or hypoautofluorescent and showing confluence toward the center of the macula.[35] Third, STGD1 flecks usually are spread diffusely across the posterior pole and middle periphery, as opposed to drusen, which are concentrated mainly in the macular area. Stargardt disease type 1 flecks are situated within the photoreceptor layers, leading to interruptions in the ELM and EZ layers.[36] In contrast, most drusen are located beneath the RPE, causing undulations and elevations in the RPE band while generally leaving the overlying inner retinal layers intact.[37] Reticular drusen share similar laminar location as flecks, but on FAF imaging, they present as isofluorescent spots accompanied by hypoautofluorescent halos.[38] Fourth, foveal involvement is more common in AMD compared with late-onset STGD1.[39] This corresponds to a lower visual acuity at baseline in AMD compared with STGD1. Although foveal sparing is very typical for late-onset STGD1, it is not an exclusive trait, because it is also seen in patients with AMD.[40] Finally, the presence of RPE atrophy disrupts the symbiotic relationship between the RPE and the choroid, giving rise to discernible choroidal changes. For instance, in most patients with STGD1, hypocyanescence on indocyanine green angiography is evident, whereas this is present in only a limited number of patients with AMD.[41] On OCT angiography, STGD1 exhibits a more pronounced reduction in choroidal flow signal within regions affected by RPE atrophy as compared with AMD.[42] However, the use of multimodal imaging, consisting of color fundus photography, FAF, and OCT, is sufficient in distinguishing between these two diseases, rendering the need for more invasive angiography techniques unnecessary. To the trained eye, unique features can be recognized, but differentiation based solely on clinical phenotype can remain difficult, and genetic analysis of the *ABCA4* gene ultimately will reveal the difference.

Study Limitations

Limitations inherent to the retrospective nature of this study exist. First, the actual onset of retinal changes precedes the onset of symptoms. Retinal changes in late-onset STGD1 typically start in the parafoveal region and may not cause notable symptoms initially. Patients seek medical attention only after they start experiencing symptoms. This makes it challenging to determine the exact age at disease onset. In

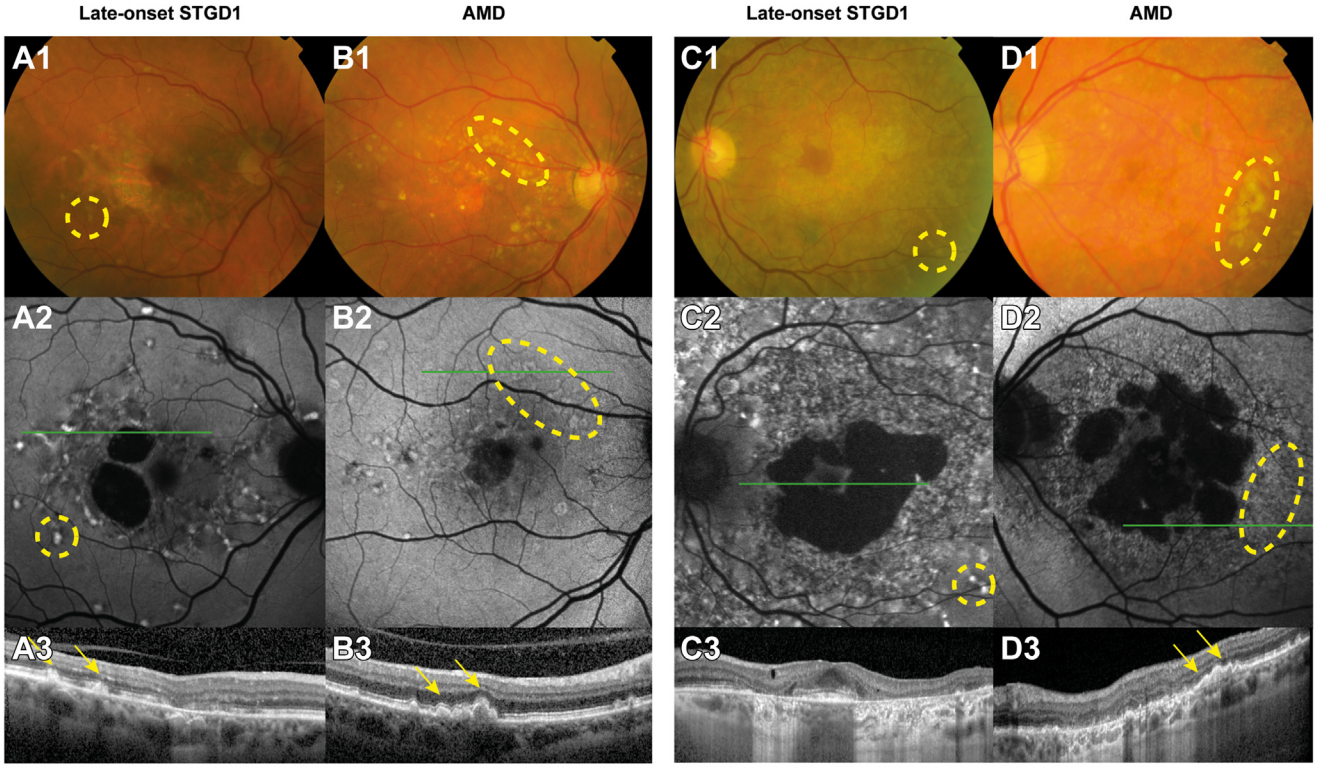

Late-onset STGD1	AMD with geographic atrophy
RPE atrophy, often foveal sparing	*Geographic atrophy, sometimes foveal sparing*
Flecks - irregular shaped (pisciform) - located diffusely in posterior pole/midperiphery	*Drusen* - round shaped - located mainly in the macular area with confluence towards the center
- CFP: slightly yellow - OCT: deposits located in the photoreceptor layers; interruptions in ELM/EZ - FAF: hyperautofluorescent	- CFP: prominenty yellow - OCT: elevations usually in RPE (sub-RPE); intact ELM/EZ - FAF: mildy increased/normal or decreased autofluorescent

Figure 7. Distinctive features that allow differentiation between late-onset Stargardt disease type 1 (STGD1) and age-related macular degeneration (AMD) based on multimodal imaging. Patient with late-onset STGD1 (**A**, **C**) with foveal-sparing retinal pigment epithelium (RPE) atrophy (**C2**) surrounded by pisciform flecks. Patient with AMD (**B**, **D**) with atrophy and round drusen. Note that drusen in AMD are very prominently yellow on color fundus photographs (CFP) (**B1**, **D1**). On fundus autofluorescence imaging (FAF), these drusen are mildly increased normal to decreased autofluorescent (**B2**, **D2**). In contrast, flecks in STGD1 are just slightly yellow and less notable (**A1**, **C1**), but on FAF imaging, these flecks are very prominently hyperautofluorescent (**A2**, **C2**). **A3**, OCT scan at the level of the green line showing that flecks correspond with depositions located in the photoreceptor layers, interrupting the overlaying ellipsoid zone (EZ) and external limiting membrane (ELM) layers. The drusen corresponds with depositions located between the RPE and Bruch membrane causing elevation in the RPE, but the overlaying inner retinal layers remain intact (**B3**, **D3**).

this and previous studies,[9,10,43] late-onset STGD1 is defined based on the age at onset of first symptoms. Additionally, asymptomatic patients with macular abnormalities at an age of 45 years or older who will demonstrate symptoms later on also were included. This approach allows for consistent classification and inclusion of patients.

Second, most of the patients whose disease could not be solved genetically via routine genetic testing underwent additional testing with techniques like smMIPs and HaloPlex-based sequencing in search of variants (48 of 71 patients). As a result, 23 of the 71 patients in this retrospective study did not undergo additional extensive genetic testing, which might have led to some uncommon variants having been missed in these patients.

Finally, imaging analyses in this study used conventional methodologies, including transfoveal OCT imaging and fleck analysis based on 30° or 55° FAF imaging. Although these analyses provide valuable insights, they do have limitations. One of these limitations is the inability to capture potential changes outside the study area. However, it is known that STGD1 flecks typically expand radially, moving foveally to peripherally, and thereby making

occurrences solely in the periphery rare.[36,44] Alternative methods such as macular retinal thickness, volume measurements, and complete RPE and outer retinal atrophy analysis on OCT, which are used commonly in AMD, are potential alternatives, but have not yet been studied in STGD1. We believe that the limitations identified, mostly related to the retrospective design of this unique cohort of patients with late-onset STGD1, are outweighed by the valuable findings presented in this study.

In conclusion, late-onset STGD1 is a subtype of STGD1 in patients with onset at 45 years of age or older. Most patients with late-onset STGD1 harbor 1 severe and 1 mild *ABCA4* variant. The phenotypical features of patients with STGD1 are at the mild end of the spectrum, with foveal sparing and presence of flecks being the most typical characteristics. Although recognition of this diagnosis has increased, many patients remain misdiagnosed. More knowledge of this subtype of STGD1 is necessary to avoid misdiagnoses with diseases with similar presentation like dry AMD with GA and with regard to therapeutic trials for both STGD1 and AMD.

Footnotes and Disclosures

Originally received: April 12, 2023.
Final revision: July 7, 2023.
Accepted: August 9, 2023.
Available online: August 19, 2023. Manuscript no. OPHTHA-D-23-00615.

[1] Department of Ophthalmology, Radboud University Medical Center, Nijmegen, The Netherlands.

[2] Donders Institute for Brain, Cognition and Behavior, Radboud University Medical Center, Nijmegen, The Netherlands.

[3] Department of Human Genetics, Radboud University Nijmegen Medical Center, Nijmegen, The Netherlands.

[4] Academic Alliance Genetics, Radboud University Medical Center, Nijmegen, and Maastricht University Medical Center+, Maastricht, The Netherlands.

Disclosure(s):

All authors have completed and submitted the ICMJE disclosures form.

The author(s) have no proprietary or commercial interest in any materials discussed in this article.

Supported by the Foundation Fighting Blindness (grant no.: PPA-0517-0717-RAD [F.P.M.C., R.W.J.C., C.B.H.]); and the Health Research Charities Ireland and the Health Research Board Joint Funding Scheme 2020-007 (to F.P.M.C.). The sponsor or funding organization had no role in the design or conduct of this research.

Presented as an abstract at: Association for Research in Vision and Ophthalmology Annual Meeting, April 2023, New Orleans, Louisiana.

HUMAN SUBJECTS: Human subjects were included in this study. All research adhered to the tenets of the Declaration of Helsinki. The insitutional ethics committee, CMO Radboudumc, ruled that approval was not required for this study and waived the requirement for informed consent.

No animal subjects were included in this study.

Author Contributions:

Conception and design: Li, Pas, Dhooge, Hoyng

Analysis and interpretation: Li, Pas, Corradi, Hitti-Malin, Hoogstede, Dhooge, Cremers, Hoyng

Data collection: Li, Pas, Hoogstede

Obtained funding: Hoyng, Cremers, Collin

Overall responsibility: Li, Pas, Corradi, Hitti-Malin, Hoogstede, Runhart, Dhooge, Collin, Cremers, Hoyng

Abbreviations and Acronyms:
ABCA4 = ATP binding cassette subfamily A member 4; **AMD** = age-related macular degeneration; **DDAF** = definitely decreased autofluorescence; **ELM** = external limiting membrane; **EZ** = ellipsoid zone; **FAF** = fundus autofluorescence; **GA** = geographic atrophy; **IQR** = interquartile range; **logMAR** = logarithm of the minimum angle of resolution; **RPE** = retinal pigment epithelium; **smMIP** = single-molecule molecular inversion probe; **STGD1** = Stargardt disease type 1; **TDAF** = total decreased autofluorescence.

Keywords:
ABCA4, Foveal sparing, Late-onset Stargardt disease, Natural history, STGD1.

Correspondence:
Carel B. Hoyng, MD, PhD, Department of Ophthalmology (696), Radboud University Medical Center, Geert Grooteplein Zuid 10, 6525 GA Nijmegen, The Netherlands. E-mail: carel.hoyng@radboudumc.nl.

References

1. Stargardt K. Über familiäre, progressive degeneration in der maculagegend des Auges. *Graefes Arch Clin Exp Ophthalmol*. 1909;(71):534–550.
2. Allikmets R, Singh N, Sun H, et al. A photoreceptor cell-specific ATP-binding transporter gene (ABCR) is mutated in recessive Stargardt macular dystrophy. *Nat Genet*. 1997;15(3):236–246.
3. Klevering BJ, Deutman AF, Maugeri A, et al. The spectrum of retinal phenotypes caused by mutations in the ABCA4 gene. *Graefes Arch Clin Exp Ophthalmol*. 2005;243(2):90–100.
4. Lambertus S, van Huet RA, Bax NM, et al. Early-onset Stargardt disease: phenotypic and genotypic characteristics. *Ophthalmology*. 2015;122(2):335–344.
5. Sangermano R, Khan M, Cornelis SS, et al. ABCA4 midigenes reveal the full splice spectrum of all reported noncanonical splice site variants in Stargardt disease. *Genome Res*. 2018;28(1):100–110.
6. Cornelis SS, Runhart EH, Bauwens M, et al. Personalized genetic counseling for Stargardt disease: offspring risk estimates based on variant severity. *Am J Hum Genet*. 2022;109(3):498–507.
7. Cremers FP, van de Pol DJ, van Driel M, et al. Autosomal recessive retinitis pigmentosa and cone-rod dystrophy caused by splice site mutations in the Stargardt's disease gene ABCR. *Hum Mol Genet*. 1998;7(3):355–362.
8. Runhart EH, Sangermano R, Cornelis SS, et al. The common ABCA4 variant p.Asn1868Ile shows nonpenetrance and

variable expression of Stargardt disease when present in trans with severe variants. *Invest Ophthalmol Vis Sci*. 2018;59(8):3220–3231.
9. Westeneng-van Haaften SC, Boon CJ, Cremers FP, et al. Clinical and genetic characteristics of late-onset Stargardt's disease. *Ophthalmology*. 2012;119(6):1199–1210.
10. Lambertus S, Lindner M, Bax NM, et al. Progression of late-onset Stargardt disease. *Invest Ophthalmol Vis Sci*. 2016;57(13):5186–5191.
11. van Huet RA, Bax NM, Westeneng-Van Haaften SC, et al. Foveal sparing in Stargardt disease. *Invest Ophthalmol Vis Sci*. 2014;55(11):7467–7478.
12. Runhart EH, Dhooge P, Meester-Smoor M, et al. Stargardt disease: monitoring incidence and diagnostic trends in The Netherlands using a nationwide disease registry. *Acta Ophthalmol*. 2022;100(4):395–402.
13. Bauwens M, Garanto A, Sangermano R, et al. ABCA4-associated disease as a model for missing heritability in autosomal recessive disorders: novel noncoding splice, cis-regulatory, structural, and recurrent hypomorphic variants. *Genet Med*. 2019;21(8):1761–1771.
14. Khan M, Cornelis SS, Pozo-Valero MD, et al. Resolving the dark matter of ABCA4 for 1054 Stargardt disease probands through integrated genomics and transcriptomics. *Genet Med*. 2020;22(7):1235–1246.
15. Zernant J, Lee W, Collison FT, et al. Frequent hypomorphic alleles account for a significant fraction of ABCA4 disease and distinguish it from age-related macular degeneration. *J Med Genet*. 2017;54(6):404–412.
16. Hitti-Malin RJ, Dhaenens CM, Panneman DM, et al. Using single molecule molecular inversion probes as a cost-effective, high-throughput sequencing approach to target all genes and loci associated with macular diseases. *Hum Mutat*. 2022;43(12):2234–2250.
17. Runhart EH, Khan M, Cornelis SS, et al. Association of sex with frequent and mild ABCA4 alleles in Stargardt disease. *JAMA Ophthalmol*. 2020;138(10):1035–1042.
18. Jaganathan K, Kyriazopoulou Panagiotopoulou S, McRae JF, et al. Predicting splicing from primary sequence with deep learning. *Cell*. 2019;176(3):535–548.e24.
19. Kuehlewein L, Hariri AH, Ho A, et al. Comparison of manual and semiautomated fundus autofluorescence analysis of macular atrophy in Stargardt disease phenotype. *Retina*. 2016;36(6):1216–1221.
20. Maheshwari SY, Chakole S. A rare occurrence of Stargardt disease in a quadragenarian adult. *Cureus*. 2022;14(10):e30859.
21. Alsberge JB, Agarwal A. Late-onset Stargardt disease. *Am J Ophthalmol Case Rep*. 2022;26:101429.
22. Hanany M, Rivolta C, Sharon D. Worldwide carrier frequency and genetic prevalence of autosomal recessive inherited retinal diseases. *Proc Natl Acad Sci U S A*. 2020;117(5):2710–2716.
23. Lee W, Zernant J, Su PY, et al. A genotype-phenotype correlation matrix for ABCA4 disease based on long-term prognostic outcomes. *JCI Insight*. 2022;7(2):e156154.
24. Collison FT, Lee W, Fishman GA, et al. Clinical characterization of Stargardt disease patients with the p.N1868I ABCA4 mutation. *Retina*. 2019;39(12):2311–2325.
25. van Driel MA, Maugeri A, Klevering BJ, et al. ABCR unites what ophthalmologists divide(s). *Ophthalmic Genet*. 1998;19(3):117–122.
26. Valkenburg D, Runhart EH, Bax NM, et al. Highly variable disease courses in siblings with Stargardt disease. *Ophthalmology*. 2019;126(12):1712–1721.
27. Fritsche LG, Fleckenstein M, Fiebig BS, et al. A subgroup of age-related macular degeneration is associated with monoallelic sequence variants in the ABCA4 gene. *Invest Ophthalmol Vis Sci*. 2012;53(4):2112–2118.
28. Curcio CA, Sloan KR, Kalina RE, Hendrickson AE. Human photoreceptor topography. *J Comp Neurol*. 1990;292(4):497–523.
29. Bax NM, Valkenburg D, Lambertus S, et al. Foveal sparing in central retinal dystrophies. *Invest Ophthalmol Vis Sci*. 2019;60(10):3456–3467.
30. Battaglia Parodi M, Sacconi R, Romano F, Bandello F. Hyperreflective foci in Stargardt disease: 1-year follow-up. *Graefes Arch Clin Exp Ophthalmol*. 2019;257(1):41–48.
31. Kong X, West SK, Strauss RW, et al. Progression of visual acuity and fundus autofluorescence in recent-onset Stargardt disease: Progstar study report #4. *Ophthalmol Retina*. 2017;1(6):514–523.
32. Shen LL, Sun M, Grossetta Nardini HK, Del Priore LV. Natural history of autosomal recessive Stargardt disease in untreated eyes: a systematic review and meta-analysis of study- and individual-level data. *Ophthalmology*. 2019;126(9):1288–1296.
33. Lim LS, Mitchell P, Seddon JM, et al. Age-related macular degeneration. *Lancet*. 2012;379(9827):1728–1738.
34. Saksens NT, Fleckenstein M, Schmitz-Valckenberg S, et al. Macular dystrophies mimicking age-related macular degeneration. *Prog Retin Eye Res*. 2014;39:23–57.
35. Schmitz-Valckenberg S, Fleckenstein M, Scholl HP, Holz FG. Fundus autofluorescence and progression of age-related macular degeneration. *Surv Ophthalmol*. 2009;54(1):96–117.
36. Sparrow JR, Marsiglia M, Allikmets R, et al. Flecks in recessive Stargardt disease: short-wavelength autofluorescence, near-infrared autofluorescence, and optical coherence tomography. *Invest Ophthalmol Vis Sci*. 2015;56(8):5029–5039.
37. Schlanitz F, Baumann B, Sacu S, et al. Impact of drusen and drusenoid retinal pigment epithelium elevation size and structure on the integrity of the retinal pigment epithelium layer. *Br J Ophthalmol*. 2019;103(2):227–232.
38. Querques G, Querques L, Martinelli D, et al. Pathologic insights from integrated imaging of reticular pseudodrusen in age-related macular degeneration. *Retina*. 2011;31(3):518–526.
39. Lindner M, Lambertus S, Mauschitz MM, et al. Differential disease progression in atrophic age-related macular degeneration and late-onset Stargardt disease. *Invest Ophthalmol Vis Sci*. 2017;58(2):1001–1007.
40. Forte R, Querques G, Querques L, et al. Multimodal evaluation of foveal sparing in patients with geographicatrophy due to age-related macular degeneration. *Retina*. 2013;33(3):482–489.
41. Giani A, Pellegrini M, Carini E, et al. The dark atrophy with indocyanine green angiography in Stargardt disease. *Invest Ophthalmol Vis Sci*. 2012;53(7):3999–4004.
42. Müller PL, Pfau M, Möller PT, et al. Choroidal flow signal in late-onset Stargardt disease and age-related macular degeneration: an OCT-angiography study. *Invest Ophthalmol Vis Sci*. 2018;59(4). AMD122–AMD31.
43. Runhart EH, Valkenburg D, Cornelis SS, et al. Late-onset Stargardt disease due to mild, deep-intronic ABCA4 alleles. *Invest Ophthalmol Vis Sci*. 2019;60(13):4249–4256.
44. Cukras CA, Wong WT, Caruso R, et al. Centrifugal expansion of fundus autofluorescence patterns in Stargardt disease over time. *Arch Ophthalmol*. 2012;130(2):171–179.